

# Airborne Particle Classification with a Combination of Chemical Composition and Shape Index Utilizing an Adaptive Resonance Artificial Neural Network

Ying Xie and Phillip K. Hopke\*

Chemistry Department, Clarkson University, Potsdam, New York 13699-5810

Dietrich Wienke

Laboratory for Analytical Chemistry, Catholic University of Nijmegen, Toernooiveld 1, 6525 ED Nijmegen, The Netherlands

Airborne particle classification that leads to particle source identification is important to both the improvement of the environment and the protection of public health. In this study, individual airborne particles were analyzed using a computer-controlled scanning electron microscope (CCSEM). It was found that a more accurate particle classification can be obtained when it is based on both the chemical compositions and a shape index of the individual particles compared to one that is based only on the chemical compositions. This study also demonstrated that a newly developed adaptive resonance artificial neural network system (ART2A) has a high potential value in particle classification. The ART2A system can identify new cluster(s) for the unknown particles and dynamically update the particle class library. Thus, it provides a way to both identify and further investigate new sources for the airborne particles.

## Introduction

Airborne particles play a very important role in air quality with the resulting problems of public health. In order to make effective control strategies, studies of particle composition, sources, and transportation are needed. Receptor models based on single-particle classification have proven to have high specificity for source identification and airborne particle mass apportionment (1, 2). However, these models depend directly on the ability to classify particles into well-defined classes. Thus, particle classification is a critical first step in the use of single-particle receptor models.

The computer-controlled scanning electron microscope (CCSEM) is a powerful tool to analyze individual particles. It can automatically scan a portion of a sample filter for individual particles and provide fluoresced X-ray and image at the same time. Currently, particle classification has been performed based only on the chemical information obtained from the fluoresced X-rays. However, some particles may share very similar chemical composition but come from different sources. For example, Figures 1 and 2 show the X-ray fluorescence spectra and the images of a clay mineral particle and a fly ash particle, respectively. From the X-ray spectra, it can be seen that the two particles have very similar chemical compositions. However, their images show that their shapes are quite different. In order to develop effective pollution control strategies, it is important to distinguish between these two sources. The fly ash particles are from combustion processes. The clay mineral particles are crustal material from natural sources. Thus, there is a need to combine a shape index with the

chemical compositions so that more accurate particle classification can be achieved.

There are many kinds of classification models. Basically, the classification models are divided into two groups. One includes supervised methods, and the other encompasses unsupervised methods. Supervised methods develop a set of rules for each well-defined class using objects whose classification are known (training set). The particles are then assigned to the classes according to their rules. Once the rules are built, they are fixed. There is no way to change them without reanalyzing the original training set. In unsupervised methods, there are no prefixed rules for each classes. Particles are divided into clusters based on a similarity matrix and a clustering criterion. The similarity measures are mainly based on a distance matrix or correlation matrix.

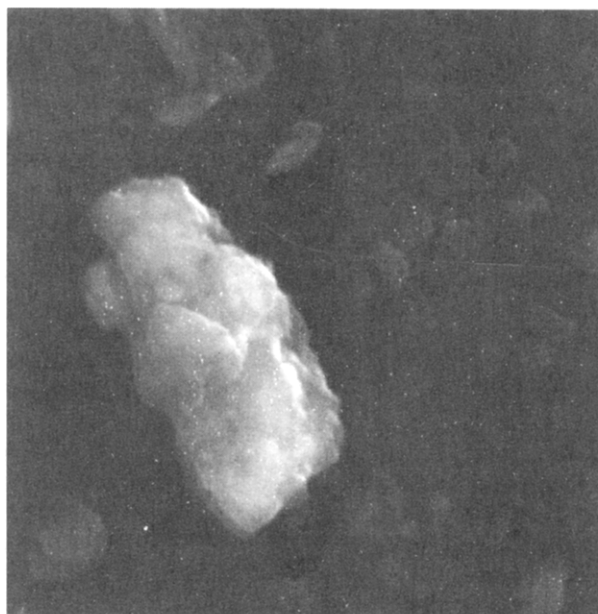
The particle class balance (PCB) model is one of the well-developed supervised model. The PCB model was developed by Hopke and Kim (1). In the PCB model, an expert system had to be developed to provide classification. The expert system is a system with a set of well-defined rules that define all the possible clusters. Then all of the particles are assigned to the corresponding clusters. However, this model cannot classify the particles that do not belong to any of the known classes. A dynamic system that could identify and establish rules for new clusters would make single-particle methods much more effective as well as easier to use.

Artificial neural networks are models that simulate the human pattern recognition system and perform pattern recognition for multiple complex signals or data. In this study, an adaptive resonance theory (ART) neural network was applied to perform the particle classification. ART is one kind of a neural network that can perform fast category learning and recognition. ART2 was first described by Grossberg (3, 4). A series of further developments were obtained by Carpenter, Grossberg, and co-workers (5-10). An application of ART to automated character interpretation has been accomplished by Gan and Lua (11). The first application in chemistry was by Wienke and Kateman (12). A modified algorithm, ART2A, was developed by Carpenter and co-workers (13) in 1991. ART2A algorithm, a variation with only one weight matrix, performs as well as the ART2 method but runs two to three times faster. It has been applied in the particle shape classification (14). ART2A can perform recognition well, and most importantly, ART2A can generate new clusters for particles with unfamiliar patterns and incorporate the rules for this new cluster in its knowledge base for the further use.

The significance of this study is that both the chemical composition information and shape index were included

\* Author to whom correspondence should be addressed; e-mail address: hopkepk@craft.camp.clarkson.edu.

### CLAY/MINERAL PARTICLE#1



4718x |-----| 5.0  $\mu$ m

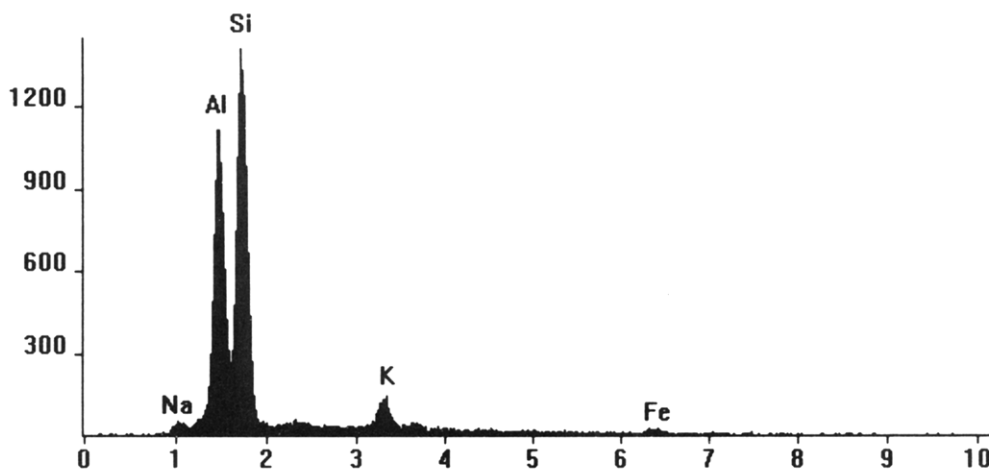


Figure 1. X-ray spectrum and image of a clay mineral particle.

in the particle classification scheme. Secondly, the newly developed artificial neural network ART2A was used so that new clusters can be dynamically generated for the particles that do not belong to the initially known classes.

#### *Principles of the ART2A Model*

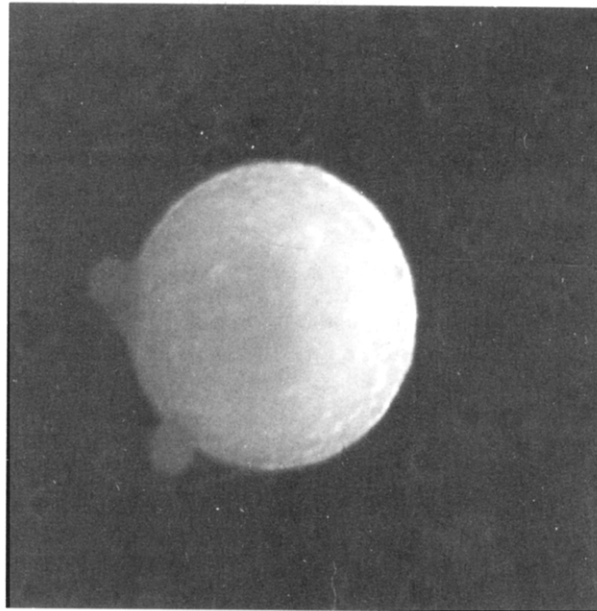
The ART2 system can simulate human pattern recognition and has some of the advanced properties that a human brain has. It is self-organizing. It has a plasticity and stability balance in building rules for the pattern recognition. *Plasticity* means that the system keeps learning from the input information until it discovers critical feature patterns or prototypes that represent an invariant of the set of all experienced input patterns. *Stability* means that the system reaches a steady state while the learned codes are dynamically buffered against relentless recording by irrelevant inputs. There is a trade off between plasticity and stability. Plasticity is important in order to learn about significant new events. However, the system must remain stable in response to irrelevant or often-repeated events. This system can preserve its

plasticity-stability balance even with substantial and highly complex input patterns.

The ART2 system is self-scaling to help identify critical feature patterns. Thus, important features can be identified even though the signal might be very small. It can self-adjust the search order. The ART2 system is capable of a parallel memory search that adaptively updates its search order to maintain efficiency as its recognition code becomes arbitrarily complex because of prior learning. It can adjust the search order such that it can remain optimal in many kinds of knowledge domains.

In addition, the ART2 system can directly access familiar patterns without going through the whole "rules" library. Finally, the ART2 system can get the environment involved in the whole processing procedure. This means that the whole processing procedure is not isolated; a vigilance parameter can be adjusted by the user depending on whether a coarse discrimination or a fine discrimination is needed in different environments. The ART2A system allows a fixed set of feature detectors to function successfully in an environment that imposes variable performance demands.

FLY ASH PARTICLE#2



10086x |-----| 2.0 um

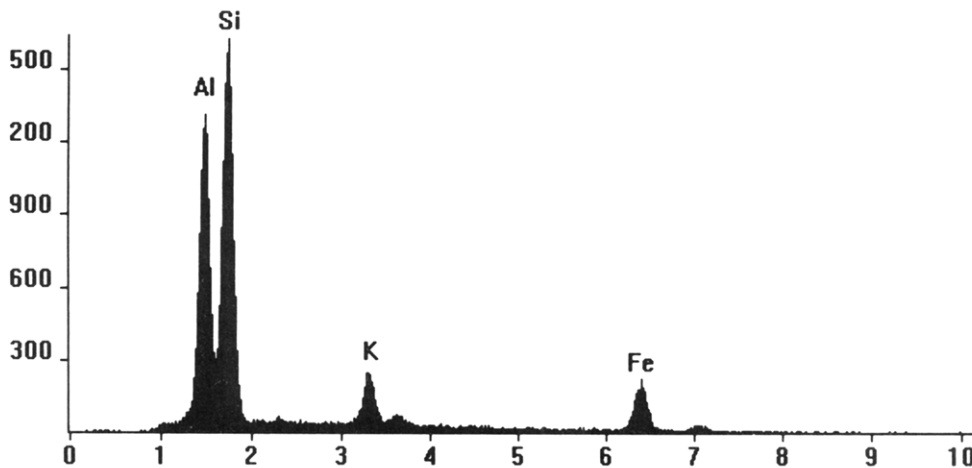


Figure 2. X-ray spectrum and image of a fly ash particle.

Figure 3 shows the structure of an ART2 system. Basically, the system contains two large parts. One portion is the *attentional subsystem* composed of the input field,  $F_1$ , and a category field,  $F_2$ . The other part is the *orienting subsystem*. The attentional subsystem processes the familiar objects while the orienting subsystem resets the attentional subsystem when an unfamiliar object is encountered. The orienting subsystem is to judge whether an object has a familiar pattern and can fall into a known cluster, or on the other hand, if it has an unknown pattern and needs to create a new recognition code. The two subsystems are connected through a bottom-up  $F_1-F_2$  adaptive filter and a up-bottom  $F_2-F_1$  adaptive filter shown in Figure 3.

An input vector generates a set of virtual outputs via a bottom-up adaptive filter. These virtual outputs describe the membership of the input vector to every distinct training class. The virtual output with the highest response (winner) is fed back via a up-bottom filter creating its individual virtual input vector in  $F_1$ . This virtual input vector is then compared with the original input vector using a similarity measure. If these two input vectors are

Orienting Subsystem      Attentional Subsystem

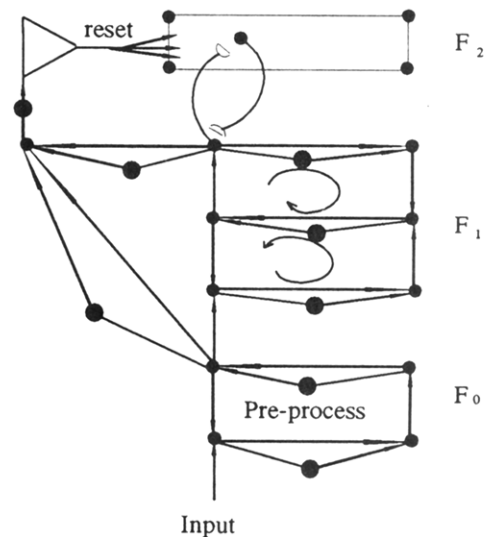


Figure 3. Diagram of the ART2A system.

similar within predefined limits, the network is in *resonance* with the original input vector. The network answers with a real output for the corresponding class. Simultaneously, the network learns this input vector by *weights adaption* for the corresponding class.

If no resonance occurred, this situation means that the neural network has discovered a *novelty*. The input vector does not fit into any of the currently known classes. The network then decides to open a new class box by an extension of the number of possible outputs (classes) and by an extension of the dimensions of the weight matrices. The network learned the detected novelty by *structure adaption*. This idea of "resonance" and "adaption" is very close to the reality of learning in human brains. This new concept promises to make the ART classifier even robust like the human brain under unexpected pattern recognition situations.

ART2A is a modified version of ART2. It emulates the self-organize recognition property of the ART2 neural network, but with a speed that is two or three times faster than the ART2 system (13). The improved speed of the ART2A algorithm is due to the explicit specification of steady-state variables as a composition of a small number of nonlinear operations (13). The steady-state equations replace a time-consuming multilayer iterative component of ART2. The algorithm used in this study is presented as follows.

**Initialization of the Network.** Suppose the raw data matrix,  $\mathbf{X}$ , consists of  $n$  row vectors,  $\mathbf{x}_i$ . Each sample is characterized by  $m$  features. A typical artificial neural network works in a way that  $c$  weight vectors,  $\mathbf{w}_i$ , of the same length as the input sample,  $m$ , are repeatedly compared with the input sample  $\mathbf{x}_m$ . During the comparison, a winner,  $\mathbf{w}_t$ , among  $c$  weight vectors can be found that has the minimum distance to the  $k$ th input vector,  $\mathbf{x}_k$ . Then the  $j = 1 \dots m$  elements  $w_{t,j,old}$  of the winning weight vector  $t$  become adapted a small step closer to the elements  $x_{ij}$  of  $\mathbf{x}_i$  using a given learning rule:

$$\mathbf{w}_k^{new} = \mathbf{w}_k^{old} + \eta(\mathbf{r}_i - \mathbf{w}_k^{old}) \quad (1)$$

where  $\mathbf{w}_k^{old}$  is the old weight vector;  $\mathbf{w}_k^{new}$  is the new weight vector;  $\mathbf{r}_i$  is the thresholded and scaled input vector; and  $\eta$  is the learning rate. After this adaption, the subset of the weight vectors becomes slightly closer to the original sample input vector. After  $N$  ( $N > 500c$ ) repetitions of comparison and adaption, a set of weight vectors are obtained with each weight vector representing one cluster of input samples.

At the initialization stage, several parameters need to be set. The threshold,  $\theta$ , is set according to  $0 < \theta < 1/(m)^{1/2}$ . This threshold is to discriminate against the noise. Signals smaller than the threshold are set to 0. Another parameter that needs to be set is the learning rate,  $\eta$ . The value of  $\eta$  determines the speed with which a weight vector is adapted toward a new input vector.  $\eta$  is set to be  $\eta < 0.5$ . Still another parameter that needs to be set is the scaling factor,  $\alpha$ . It is set as  $\alpha < 1/(m)^{1/2}$ . The class box size  $\rho$  is set according to

$$0 < \rho_{max} < 1 \quad (2)$$

$\rho$  is the cosine of the radial angle describing the unit size for all class boxes. If the angle between a sample and the weight vector is smaller than  $\arccos(\rho)$  of a particular class, this sample is in *resonance*. The last important parameter

that needs to be determined is the number of weight vectors. Assume  $c$  is the number of classes expected by the user in the training and test data sets. The number of weight vectors is  $c_{max}$ , a number larger than  $c$ . 30 was used as  $c_{max}$  in this study. The  $mc_{max}$  elements of the weight matrix  $\mathbf{W}$  are set as  $w_{j,k} = 1/(m)^{1/2}$ , whereby  $k = 1 \dots c_{max}$ .

### Training Phase of the Network.

- (1) Randomly select an input vector  $\mathbf{x}_i$  from  $\mathbf{X}$ .
- (2) Scale  $\mathbf{x}_i$  to unit length:

$$\mathbf{p}_i = \mathbf{x}_i / \|\mathbf{x}_i\| \quad (3)$$

- (3) Contrast enhancement: transfer all elements of  $\mathbf{p}_{ij}$  through a nonlinear transfer function by thresholding

$$\mathbf{q}_{ij} = \begin{cases} \mathbf{p}_{ij}, & \text{if } \mathbf{p}_{ij} > \theta \\ 0, & \text{otherwise} \end{cases} \quad (4)$$

or as one of the possible alternative functions by a sigmoidal transfer function

$$\mathbf{q}_{ij} = 1/[1 + \exp(-\mathbf{p}_{ij})] \quad (5)$$

- (4) Rescale to unit length:

$$\mathbf{r}_i = \mathbf{q}_i / \|\mathbf{q}_i\| \quad (6)$$

- (5) Evaluate the competition among all  $c$  output neurons:

$$\rho_i = \begin{cases} \alpha \sum_j \mathbf{r}_{ij}, & \text{if } k = c + 1 \\ \mathbf{r}_i \mathbf{w}_k, & \text{if } k < c + 1 \end{cases} \quad (7)$$

$$\rho_{winner} = \max(\rho_i) \quad (8)$$

- (6) Perform the resonance check and the novelty detection:

$$c = \begin{cases} c + 1, & \text{if } \rho_{winner} < \rho_{max} \\ c + 0, & \text{otherwise} \end{cases} \quad (9)$$

- (7) Network learning by weights adaption and/or structure adaption:

$$\mathbf{w}_k^{new} = \begin{cases} \mathbf{r}_i, & \text{if } \rho_{winner} < \rho_{max} \\ \mathbf{s}_k, & \text{eqs 11-14, otherwise} \end{cases} \quad (10)$$

where

$$\mathbf{s}_k = \mathbf{t}_k / \|\mathbf{t}_k\| \quad (11)$$

with

$$\mathbf{t}_k = \mathbf{u}_i + (1 - \eta)\mathbf{w}_k^{old} \quad (12)$$

$$\mathbf{u}_k = \eta \mathbf{v}_i / \|\mathbf{v}_i\| \quad (13)$$

$$\mathbf{v}_{jk} = \begin{cases} \mathbf{r}_{ij}, & \text{if } \mathbf{w}_k^{old} > \theta \\ 0, & \text{otherwise} \end{cases} \quad (14)$$

### Test Phase of the Network.

- (1) Examine data row vector of an unknown test sample  $\mathbf{x}_{unknown}$ , characterized by  $j = 1 \dots m$  features, columnwise autoscaled by parameters estimated from training set: set threshold  $0 < \theta < 1/(m)^{1/2}$ , set learning rate  $\eta < 0.5$ ; set scaling factor  $\alpha < 1/(m)^{1/2}$ ; set desired class box size  $\rho$  according to  $0 < \eta < 1$ .

- (2) For testing objects that belong to known classes: use eqs 3-14 with  $\mathbf{x}_{unknown}$  as input vector.

(3) For testing objects that do not belong to known classes: use eqs 3–8 with  $x_{\text{unknown}}$  as input vector.

### Data Description

An arbitrary set of particles collected on several ambient particle sample filters were examined using a computer-controlled scanning electron microscope (CCSEM) (15). This system can automatically scan the portion of a filter on a stub and provide the chemical composition and image of the individual particles. X-ray intensities for 20 elements for 92 particles were determined. The elements were as follows: Na, Mg, Al, Si, P, S, Cl, K, Ca, Ti, V, Cr, Mn, Fe, Co, Ni, Cu, Zn, As, and Pb.

In order to emphasize the profiles of the particle compositions, the first derivative matrix was used instead of the raw fluoresced X-ray count matrix. Considering a data array as a map, every number in the data array indicates the height of that point; thus, the whole data array represents the topology. The derivative matrix may enhance the features of this map. This technique in image processing is called an enhance filter (16). This is the theoretical basis for using the derivative matrix. In this study, an experiment was also conducted to ensure that the use of the derivative matrix would obtain a better classification than the use of the raw data matrix. The experiment did prove this point, and the model that was used to perform this experiment was another neural network, the Tree-Map model (17). Suppose  $x_{ij}$  is an element of the  $m \times n$  composition matrix and  $y_{ij}$  is the element of the first derivative matrix,  $y_{ij} = x_{ij} - x_{i,j+1}$ , then dimension of the derivative matrix is  $m \times (n - 1)$ . Thus, in this study, the dimension of the chemical information matrix is  $92 \times 19$ .

The shape index was obtained using the newly developed chain code histogram method (18). As stated in the Introduction, the major purpose of including the shape index in the model was to distinguish spherical particles from nonspherical particles. The chain code histogram method sets a criterion on the chain code histogram pattern for spherical particles and uses this criterion to examine each particle to determine if the particle is spherical. In the initial study, the frequencies of chain codes were attempted to be used to code shapes. However, the result was not satisfactory. The reason for this poor performance was that when the chain code histogram method was used to discriminate spherical particles from nonspherical ones, it is the zig-zag pattern of the histogram that has the discriminating power, not the frequencies themselves. For example, histogram vector 0.1, 0.4, 0.3, 0.5, 0.2, 0.3, 0.1 represents a spherical shape. On the other hand, vector 0.4, 0.5, 0.1, 0.3, 0.1, 0.4, 0.3 also represents a spherical shape because both of them have a zig-zag pattern. However, if these two vectors were used in the model, the result may imply that these two objects do not belong to the same group. Thus, the final choice was to use arbitrary vectors or numbers to code the shape.

One direct option was to code all the spherical particles as 1 and to code all the nonspherical particles as 0. However, if only one variable was used as the shape index, this single variable will be downweighted compared with the other 19 chemical variables because the shape index has too small a weight relative to the other 19 variables. Test studies also demonstrated that if only one shape variable was used, fly ash particles could not be distin-

guished from the clay mineral particles because their similarity in the chemical composition still dominated the classification process. Therefore, the final choice for coding the shape was to use six variables instead of using just one variable. The spherical particles were coded as 0.2, -0.2, -0.2, 0.0, 0.0, 0.2; all the nonspherical particles were coded as -0.2, 0.0, 0.2, -0.2, 0.2, 0.0.

Thus, the data matrix used in this study was 92 particles by 25 feature variables. Each row was scaled to unit length by eq 15:

$$y'_{ij} = \frac{y_{ij}}{\left(\sum_j y_{ij}^2\right)^{1/2}} \quad (15)$$

### Application of the ART2A Neural Network

**Parameters of Neural Network.** The threshold,  $\theta$ , was set to be  $0.9 \times 1/(m)^{1/2}$ . The learning rate,  $\eta$ , was set as 0.1. The parameter,  $\rho$ , that defines the class box size was set as 0.2. The maximum class number was set to be 30. This number is not the fixed number of classes, but only provides the maximum number of classes. The real number of classes is determined by the model itself based on the class box size,  $\rho$ . In this way, objects may be reasonably classified. Although sometimes a group of particles might be divided into two classes. Later, they still can be considered as belonging to one group based on the diagnostic matrix.

**Particle Classification Based Only on Chemical Compositions.** To begin this study, only the chemical compositions were included in the analysis (run I). This analysis was performed by taking all the 92 particles as the training data. After the training, the system developed a set of rules for the different clusters and stored these rules. Then, these 92 particles were used as the test data, and each particle was assigned to a known class. The results are shown in Table 1. Eight classes were identified. Cluster 1 is corresponding to the Mg-Si particles. Class 2 is for the Pb particles. Fly ash and the clay mineral particle were grouped together as cluster 3. Ti particles were assigned to class 5. Classes 4 and 6–8 were poorly defined classes. One particle (no. 34) of the 29 Mg-Si particles was classified as an outlier. Two of the 27 Pb particles (nos. 54 and 58) were identified as outliers. There was some classification noise in the fly ash and clay mineral cluster. It should be noted that there was no clear separation between fly ash and clay mineral particles.

**Particle Classification Based on both Chemical Compositions and Shape Index.** The second run (run II) was conducted by taking all 92 particles with both chemical compositions and the shape index as the training data. The results are shown in Table 2. Eight classes were again identified. Class 1 corresponds to the Pb particles. Class 2 contains the Mg-Si particles. Classes 3 and 5 are the clay mineral particles. Class 6 is the fly ash particles. Ti particles were assigned to class 4. Classes 7 and 8 were the poorly defined classes. All of the 12 Ti particles and the 11 fly ash particles were correctly classified. One particle (no. 34) of the 29 Mg-Si particles was again an outlier of this cluster. Three of the 27 Pb particles (nos. 53, 54, and 58) were misclassified: one was misassigned into the fly ash cluster, and the other two were separated from the Pb cluster as outliers. Almost all

**Table 1. Results for Run I**

particle no.	type	classification	particle no.	type	classification
1	Mg-Si	1	47	Ti	5
2	Ti	5	48	Pb	2
3	Mg-Si	1	49	Pb	2
4	Ti	5	50	Pb	2
5	Mg-Si	1	51	Pb	2
6	Mg-Si	1	52	Pb	2
7	Ti	5	53	Pb	2
8	Ti	5	54	Pb	8
9	Mg-Si	1	55	Pb	2
10	Mg-Si	1	56	Pb	2
11	Mg-Si	1	57	Pb	2
12	Mg-Si	1	58	Pb	8
13	Mg-Si	1	59	Pb	2
14	Ti	5	60	Pb	2
15	Mg-Si	1	61	Pb	2
16	Mg-Si	1	62	Pb	2
17	Mg-Si	1	63	Pb	2
18	Mg-Si	1	64	Pb	2
19	Mg-Si	1	65	Pb	2
20	Mg-Si	1	66	Pb	2
21	Ti	5	67	Pb	2
22	Mg-Si	1	68	Ti	5
23	Mg-Si	1	69	Ti	5
24	Mg-Si	1	70	fly ash	3
25	Ti	5	71	fly ash	3
26	Mg-Si	1	72	fly ash	6
27	Mg-Si	1	73	fly ash	3
28	Mg-Si	1	74	fly ash	3
29	Mg-Si	1	75	fly ash	3
30	Mg-Si	1	76	fly ash	3
31	Mg-Si	1	77	fly ash	3
32	Mg-Si	1	78	fly ash	3
33	Mg-Si	1	79	fly ash	3
34	Mg-Si	4	80	fly ash	3
35	Mg-Si	1	81	clay	3
36	Mg-Si	1	82	clay	6
37	Ti	5	83	clay	3
38	Ti	5	84	clay	6
39	Mg-Si	1	85	clay	3
40	Pb	2	86	clay	3
41	Pb	2	87	clay	6
42	Pb	2	88	clay	3
43	Pb	2	89	clay	3
44	Pb	2	90	clay	4
45	Pb	2	91	clay	3
46	pb	2	92	clay	7

of the clay particles were found to belong to classes 3 and 5. Only one particle (no. 90) was classified in cluster 8, a poorly defined cluster. Table 3 provides a diagnosis of this run. It shows the cosine of the angle between the two vectors that represent two different clusters. The larger the cosine value, the closer the two classes are to one another. From Table 3, it can be seen that the cosine value between clusters 3 and 5 is 0.36. This value is relatively large in such a diagnostic matrix. This result implies that all of the clay mineral particles were reasonably well grouped together.

The only difference between run I and run II was that run II not only included the chemical compositions but also included the shape index. The results showed that, once both the chemical compositions and the shape index were included in the analysis, a more accurate classification was obtained.

The third run (run III) was conducted such that all the particles excluding the 27 Pb particles were taken as the training data. Then the whole data set was treated as a test data set. After the training process, six classes were

**Table 2. Results for Run II**

particle no.	type	classification	particle no.	type	classification
1	Mg-Si	2	47	Ti	4
2	Ti	4	48	Pb	1
3	Mg-Si	2	49	Pb	1
4	Ti	4	50	Pb	1
5	Mg-Si	2	51	Pb	1
6	Mg-Si	2	52	Pb	1
7	Ti	4	53	Pb	6
8	Ti	4	54	Pb	7
9	Mg-Si	2	55	Pb	1
10	Mg-Si	2	56	Pb	1
11	Mg-Si	2	57	Pb	1
12	Mg-Si	2	58	Pb	7
13	Mg-Si	2	59	Pb	1
14	Ti	4	60	Pb	1
15	Mg-Si	2	61	Pb	1
16	Mg-Si	2	62	Pb	1
17	Mg-Si	2	63	Pb	1
18	Mg-Si	2	64	Pb	1
19	Mg-Si	2	65	Pb	1
20	Mg-Si	2	66	Pb	1
21	Ti	4	67	Pb	1
22	Mg-Si	2	68	Ti	4
23	Mg-Si	2	69	Ti	4
24	Mg-Si	2	70	fly ash	6
25	Ti	4	71	fly ash	6
26	Mg-Si	2	72	fly ash	6
27	Mg-Si	2	73	fly ash	6
28	Mg-Si	2	74	fly ash	6
29	Mg-Si	2	75	fly ash	6
30	Mg-Si	2	76	fly ash	6
31	Mg-Si	2	77	fly ash	6
32	Mg-Si	2	78	fly ash	6
33	Mg-Si	2	79	fly ash	6
34	Mg-Si	8	80	fly ash	6
35	Mg-Si	2	81	clay	3
36	Mg-Si	2	82	clay	5
37	Ti	4	83	clay	3
38	Ti	4	84	clay	5
39	Mg-Si	2	85	clay	3
40	Pb	1	86	clay	3
41	Pb	1	87	clay	5
42	Pb	1	88	clay	5
43	Pb	1	89	clay	3
44	Pb	1	90	clay	8
45	Pb	1	91	clay	5
46	Pb	1	92	clay	5

**Table 3. Diagnosis for Run 11**

class	1	2	3	4	5	6	7	8
1	1.00	-0.24	-0.17	0.00	-0.74	0.00	0.007	0.002
2		1.00	-0.25	0.00	-0.23	0.00	-0.008	-0.01
3			1.00	-0.002	0.36	-0.003	-0.002	-0.04
4				1.00	-0.002	0.00	-0.006	-0.27
5					1.00	-0.003	-0.005	0.004
6						1.00	-0.01	-0.02
7							1.00	-0.003
8								1.00

found. In the testing process, an additional class was discovered, and all the 27 Pb particles in the test set fell into this new cluster. The results are shown in Table 4. There was one Mg-Si particle (no. 34) that was classified as an outlier of this cluster. One fly ash particle (no. 73) was misassigned to the clay mineral class. Similar to the result of run II, the clay mineral particles were assigned to two clusters. The diagnostics in Table 5 show that these two clusters are very close with a cosine value of 0.34. One particle (no. 90) was classified as an outlier of this cluster.

**Table 4. Results for Run III**

particle no.	type	classification	particle no.	type	classification
1	Mg-Si	1	47	Ti	2
2	Ti	2	48	Pb	7
3	Mg-Si	1	49	Pb	7
4	Ti	2	50	Pb	7
5	Mg-Si	1	51	Pb	7
6	Mg-Si	1	52	Pb	7
7	Ti	2	53	Pb	7
8	Ti	2	54	Pb	7
9	Mg-Si	1	55	Pb	7
10	Mg-Si	1	56	Pb	7
11	Mg-Si	1	57	Pb	7
12	Mg-Si	1	58	Pb	7
13	Mg-Si	1	59	Pb	7
14	Ti	2	60	Pb	7
15	Mg-Si	1	61	Pb	7
16	Mg-Si	1	62	Pb	7
17	Mg-Si	1	63	Pb	7
18	Mg-Si	1	64	Pb	7
19	Mg-Si	1	65	Pb	7
20	Mg-Si	1	66	Pb	7
21	Ti	2	67	Pb	7
22	Mg-Si	1	68	Ti	2
23	Mg-Si	1	69	Ti	2
24	Mg-Si	1	70	fly ash	6
25	Ti	2	71	fly ash	6
26	Mg-Si	1	72	fly ash	6
27	Mg-Si	1	73	fly ash	3
28	Mg-Si	1	74	fly ash	6
29	Mg-Si	1	75	fly ash	6
30	Mg-Si	1	76	fly ash	6
31	Mg-Si	1	77	fly ash	6
32	Mg-Si	1	78	fly ash	6
33	Mg-Si	1	79	fly ash	6
34	Mg-Si	5	80	fly ash	6
35	Mg-Si	1	81	clay	3
36	Mg-Si	1	82	clay	4
37	Ti	2	83	clay	3
38	Ti	2	84	clay	4
39	Mg-Si	1	85	clay	3
40	Pb	7	86	clay	3
41	Pb	7	87	clay	3
42	Pb	7	88	clay	3
43	Pb	7	89	clay	3
44	Pb	7	90	clay	5
45	Pb	7	91	clay	4
46	Pb	7	92	clay	4

**Table 5. Diagnosis for Run III**

class	1	2	3	4	5	6	7
1	1.00	-0.14	-0.61	-0.35	-0.01	0.21	-0.002
2		1.00	-0.20	-0.001	-0.26	-0.47	-0.001
3			1.00	0.34	-0.02	0.47	0.01
4				1.00	-0.17	0.00	-0.001
5					1.00	-0.04	0.04
6						1.00	-0.01
7							1.00

The most interesting result obtained from run III was that the unfamiliar pattern of the lead particles in the test set was discovered as a new cluster during the testing process. Moreover, the fly ash and clay mineral particles were still separated as two classes.

The fourth run (run IV) was performed such that there were 50 particles in the training set, and the other 42 particles were the test set. In the training set, there were a number of particles for every class type except for the lead class. In the test set, there were several particles for every particle class including the lead particles. Seven clusters were found during the training process. After the

**Table 6. Results for Run IV**

particle no.	type	classification	particle no.	type	classification
1	Mg-Si		47	Ti	5
2	Ti		48	Pb	8
3	Mg-Si		49	Pb	8
4	Ti		50	Pb	8
5	Mg-Si		51	Pb	8
6	Mg-Si		52	Pb	8
7	Ti		53	Pb	8
8	Ti		54	Pb	8
9	Mg-Si		55	Pb	8
10	Mg-Si		56	Pb	8
11	Mg-Si		57	Pb	8
12	Mg-Si		58	Pb	8
13	Mg-Si		59	Pb	8
14	Ti		60	Pb	8
15	Mg-Si		61	Pb	8
16	Mg-Si		62	Pb	8
17	Mg-Si		63	Pb	8
18	Mg-Si		64	Pb	8
19	Mg-Si		65	Pb	8
20	Mg-Si		66	Pb	8
21	Ti		67	Pb	8
22	Mg-Si		68	Ti	5
23	Mg-Si		69	Ti	5
24	Mg-Si		70	fly ash	3
25	Ti		71	fly ash	3
26	Mg-Si		72	fly ash	3
27	Mg-Si		73	fly ash	3
29	Mg-Si		74	fly ash	3
29	Mg-Si		75	fly ash	3
30	Mg-Si		76	fly ash	3
31	Mg-Si		77	fly ash	3
32	Mg-Si		78	fly ash	3
33	Mg-Si		79	fly ash	3
34	Mg-Si		80	fly ash	3
35	Mg-Si	4	81	clay	
36	Mg-Si	4	82	clay	1
37	Ti	5	83	clay	
38	Ti	5	84	clay	1
39	Mg-Si	4	85	clay	
40	Pb	8	86	clay	
41	Pb	8	87	clay	1
42	Pb	8	88	clay	
43	Pb	8	89	clay	
44	Pb	8	90	clay	
45	Pb	8	91	clay	
46	Pb	8	92	clay	

testing process, one additional class was identified, and all of the lead particles in the test set were assigned to this class. Table 6 shows the results. All of the particles in this table with an assignment to a class were in the test set, and all of the other particles were in the training set. It can be seen that all of the particles were well classified and there were no outliers for any class. From the diagnostic matrix, it was found that classes 1 and 4 were close to each other with the cosine value of 0.46. This result can be explained by the similar pattern of these two clusters. From Table 6, it can be seen that class 1 was for the clay mineral particles and class 4 was for the Mg-Si particles. Because the clay mineral particles also contain a high percentage of Si, these two types of particles do have similar chemical compositions. Furthermore, both of these two types of particles are nonspherical in shape. Therefore, these two classes had the strongest correlation among all the eight clusters.

The significance of run IV was that the training data set and the test set were independent from each other. The ART2A system still was able to identify the new cluster,

and all the particles in the test set were correctly assigned to their corresponding classes.

#### *Discussions of the Outliers*

In the results of the first three runs, particle nos. 34 and 90 were identified as outliers in every run, and they each always belonged to a single class. After the original data were examined, it was found that particle no. 34 has a relatively large Ca value while the other Mg-Si particles do not contain Ca. Therefore, particle no. 34 was found to be a true outlier. Particle no. 90 also contains a relatively high Ca concentration compared to the other clay mineral particles. Thus, particle no. 90 was identified as an outlier from the clay mineral clusters. Moreover, since clay mineral particles also show a high count rate for Si counts as Mg-Si particles do, particle nos. 34 and 90 were always found in the same class as the outliers of their own clusters. The other common outliers were particle nos. 54 and 58. They were the outliers from the Pb cluster. All of the Pb particles contained more than 85% Pb with no Zn. However, particle nos. 54 and 58 contained Pb and Zn, making them outliers from the Pb class.

#### *Conclusions*

This study obtained a more accurate particle classification by combining the chemical compositions and a shape index. Fly ash and clay mineral particles that are chemically similar were successfully separated. This study also demonstrated that the newly developed ART2A artificial neural network has a high potential value in particle classification. Its advantage lies in the fact that the particle class library can be dynamically updated. This point has its practical importance because it aids in the identification of new sources for the airborne particles. In the PCB or most other previously used models, the particles that do not belong to the known class will be assigned to a miscellaneous class, and no further information can be obtained. However, the ART2A system can identify new cluster(s) for the unknown particles and can provide the pattern for the new cluster(s). Thus, it provides a way to both identify and further investigate their sources.

#### *Acknowledgments*

We wish to thank Mr. Gary Casuccio and Mr. Brad Henderson for their efforts in providing the CCSEM data

for the particles. This work has been supported by the National Science Foundation under Grants ATM 8996203 and ATM 9114750.

#### *Literature Cited*

- (1) Kim, D.; Hopke, P. K. *Aerosol Sci. Technol.* **1988**, *9*, 133-151.
- (2) Kim, D.; Hopke, P. K. *Aerosol Sci. Technol.* **1988**, *9*, 221-235.
- (3) Grossberg, S. *Biol. Cybernetics* **1976**, *23*, 121-134.
- (4) Grossberg, S. *Biol. Cybernetics* **1976**, *23*, 187-203.
- (5) Grossberg, S. *The Adaptive Brain I-Cognition, Learning, Reinforcement and Rhythm*; North Holland Publisher: Amsterdam, 1987; *Advances in Psychology Series*, Vol. 42, pp 85-86, 117-118, and 189-190.
- (6) Grossberg, S. *The Adaptive Brain II-Cognition, Learning, Reinforcement and Rhythm*; North Holland Publisher: Amsterdam, 1987; *Advances in Psychology Series*, Vol. 43, pp 313-440.
- (7) Carpenter, G. A.; Grossberg, S. *Appl. Optics* **1987**, *12* (1) 4919-4930.
- (8) Carpenter, G. A.; Grossberg, S. *IEEE Comput.* **1988**, *21* (3), 77-78.
- (9) Carpenter, G. A.; Grossberg, S. *Neural Networks* **1990**, *3* (2), 129-152.
- (10) Carpenter, G. A.; Grossberg, S.; Reynolds, J. H. *Neural Networks* **1991**, *4*, 565-588.
- (11) Gan, K. W.; Lua, K. T. *Pattern Recognit.* **1992**, *25* (8), 877-882.
- (12) Wienke, D.; Kateman, G. *Chemom. Intell. Lab. Syst.* **1994**, *23*, 309-329.
- (13) Carpenter, G. A.; Grossberg, S.; Rosen, D. B. *Neural Networks* **1991**, *4* (4), 493-504.
- (14) Wienke, D.; Xie, Y.; Hopke, P. K. *Chemom. Intell. Lab. Syst.*, in press.
- (15) Casuccio, G. S.; Janocko, P. B.; Lee, R. J.; Kelly, J. F.; Dattner, S. L.; Mgebroff, J. S. *JAPCA* **1983**, *33*, 937.
- (16) Berthold, K. P. H. *Robot Vision*, 1st ed.; MIT Press: Cambridge, 1986; Chapter 8, pp 161-163.
- (17) Wienke, D.; Xie, Y.; Hopke, P. K. Submitted to *Anal. Chim. Acta*.
- (18) Xie, Y.; Hopke, P. K.; Casuccio, G.; Henderson, B. The Use of Chain Code Histogram to Quantify Individual Airborne Particle Shapes. *Aerosol Sci. Technol.*, in press.

Received for review February 7, 1994. Revised manuscript received June 17, 1994. Accepted June 27, 1994.\*

\* Abstract published in *Advance ACS Abstracts*, August 1, 1994.